FACTA UNIVERSITATIS
Series: **Physics, Chemistry and Technology** Vol. 6, Nº 1, 2008, pp. 11 - 28
DOI: 10.2298/FUPCT0801011V

COMPLEX ANALYTIC SIGNALS APPLIED ON TIME DELAY ESTIMATION

UDC 621.39;181;618;392

Zoran S. Veličković[1], Vlastimir D. Pavlović[2]

[1]Department of Electronic Engineering, High Technical School, Aleksandra Medvedeva 20, 18000 Niš, Serbia, zorvel@bankerinter.net
[2]Faculty of Electronic Engineering, Aleksandra Medvedeva 14, 18000 Niš, Serbia, vpavlovic@elfak.ni.ac.yu

Abstract. *In this paper, we present the concept of the time delay estimation based on the transformation of real sensor signals into analytic ones. We analyze the differential time delay values obtained using real seismic signals, simulated complex analytic signals and simulated complex analytic signals with real parts coming from real seismic signals. The simulation results indicate that the application of complex analytic signals leads to reliable computation of the differential time delay. The influence of specific signal parameters on spectral coherence threshold in systems for passive localization and proposed methods for lowering the threshold is analyzed. The computation of all differential time delays with respect to the reference sensor (geophone) is based on the application of Generalized Cross-Correlation (GCC) applied on corresponding analytic signals. The difficulties to select a peak of cross-correlation function that corresponds to true differential time delay when dealing with real signals are significantly reduced if GCC is applied on analytic signals. The efficiency of the proposed technique on differential delay estimation is performed on deterministic and real-life signals.*

Key words: *Array signal processing, complex analytic signal, differential time delay, generalized cross-correlation, source localization, spectral coherence*

1. INTRODUCTION

The localization of the signal source using passive sensors is applied in various fields. Source bearing and range estimation is one application of Time Delay Estimation (TDE). The most important parameters in passive source localization are propagation velocity of waves and differential time delay of signals. To perform passive seismic source localization [1], [2], it is necessary to determine the propagation velocity seismic waves [3] and the difference time delay of the signals. The differential time delay can be obtained using real seismic signals or simulated complex analytic signals [4] with real parts coming from real seismic signals. The techniques developed for acoustic signal processing can be suc-

Received February 19, 2008

cessfully adapted for application of passive localization of seismic wave sources. The efficiency circle method can be used for determination of the source coordinates in the explicit form [5]. Thus, acoustic signals, with well-known propagation velocity in the air, can be efficiently utilized not only for vehicle localization, but also for determination of their motion speed. Composed method can be used in passive source localization systems with multiple distributed sub arrays to estimate TDE between the widely separated sensors [6]. In order to simultaneously track trajectories of several acoustic sources, *ad hoc* sensor arrays that make possible source localization based on signal energy measurements can be formed [7]. Passive localization can be implemented in intelligent systems for detection, tracking and classification (recognition) type of sources [8]. Another very useful application, which uses similar methods, is passive localization of the fracture source in materials [9].

Systems for active localization can also use similar signal processing methods. In sonar-based systems, processing of sensor signals, obtained from hydrophones and used for underwater acoustic sources location, is performed [10]. The existing methods for source localization are based on the measurement of the following variables: TDE (time delay estimation between widely separated sensors), DOA (direction of arrival) [11], [12] and energy of received signal. TDE is applied at localization of wide-band signal sources. This method is considered in detail in [12]-[15]. The estimation of time delay using phase measurements is discussed in [16]. This method is also recommended for wide-band source localization. The boundaries for accuracy of passive localization of moving sources are discussed in [17]-[20]. The major goal of this research was to minimize variance (the random error) of differential time delay computation in the presence of statistically independent noise at the receiver. The research is then extended to the computation of the number of signal sources [21]-[22] and time delay estimation when the number of sources is larger than the number of sensors in the sensor array. This technique is based on high order spectra computation of the receiver sensor signals [23]. The main motivation to use higher order spectra is the lack of Gaussian noise influence. Computation of differential time delay among two received sensor signals is very important when wave propagation velocity of signal source position is determined. A lot of algorithms presented to determine differential delay are based on the cross-correlation function of sensor signals. A method to determine differential delay based on FIR coefficient computation of one of the signals is presented in [24]. FIR filter coefficients are determined by minimizing the mean square error between the filtered signal and the other signal.

The high-resolution method MUSIC is based on the eigen-decomposition of the sample covariance matrix of the received data by passive array sensors. In the case of imperfect signal coherence, the computation of the angle of arrival using high-resolution methods significantly degrades. If *a priori* characteristics of the spatial coherence matrix are known, the influence of imperfect coherence can be significantly reduced. To resolve this problem, the technique of matrix fitting is recommended [12].

The paper is organized as follows. In Section II, we present the cross-correlation method and formulate the coherence and magnitude square coherence functions. Based on these functions, the threshold of spectral coherence, which has to be achieved to perform reliable determination of differential time delay between signals, is considered. Section III contains an analytical data model of signal and signal parameters. The signals are modeled based on complex exponential polynomials. The waveforms of real-life experimental and deterministic sensor signals are presented. In Section IV, the efficiency of

the proposed technique on simulated deterministic signals is tested. For several examples of known differential time delay, we display the results obtained for the real part of a simulated signal and for a complex analytic signal. Real and imaginary parts of the complex simulated signal, connected by the Hilbert transformation, are depicted. The connection between real and imaginary parts of the complex signal is utilized when the method is tested on real-life signals. Namely, by application of the Hilbert transformation on geophone signals, a complex analytic signal is obtained, which is necessary to apply the proposed method. Simulated analytic signals correspond to the geophone signals with an eigen-frequency (resonant frequency) of 16Hz and are represented by quadratic complex polynomials. The influence of differential time delay magnitude on the accuracy is illustrated at signal to noise ratio of 10dB.

2. TIME DELAY ESTIMATION (TDE)

A The Basics of Cross-correlation

The signals considered here originate from remote seismic sources and are picked up by geophones in noise environment. We assume that $s_1(t)$ and $s_2(t)$ are two spatially separated sensors' outputs and that they can be mathematically modeled as:

$$s_1(t) = s(t) + n_1(t) \tag{1}$$

$$s_2(t) = as(t + D) + n_2(t) \tag{2}$$

where $s(t)$, $n_1(t)$ and $n_2(t)$ are real valued jointly stationary random Gaussian processes. The parameter is the attenuation (scale) factor and D is the value of differential time delay. The characteristics of signal and noise remain stationary for finite observation time. The signal $s(t)$ is uncorrelated with the noise $n_1(t)$ and $n_2(t)$. Another important condition is that D and the correlation length (inverse bandwidth) of the signal and the noise are much smaller than the observation time. The signal $as(t + D)$ is a shifted and scaled version of the unknown signal $s(t)$. The basic approach to estimate the differential time delay is to shift the signal $s_1(t)$ with respect to the signal $s_2(t)$ and to look for the similarities between them. The best agreement will occur at a shift equal to D. The well known method for determining the differential time delay is to compute the cross-correlation function [13]:

$$R_{s_1 s_2}(\tau) = E\{s_1(t)s_2(t + \tau)\} = aR_{ss}(\tau - D) + R_{n_1 n_2}(\tau) \tag{3}$$

where τ is a variable time, $E\{\bullet\}$ is expectation, $R_{ss}\{\bullet\}$ is the autocorrelation function of $s(t)$, and $R_{n_1 n_2}\{\bullet\}$ is the cross-correlation of noise. If $n_1(t)$ and $n_2(t)$ are mutually independent processes then $R_{n_1 n_2}(\tau) = 0$. The time delay D can be estimated when the maximizing function $R_{s_1 s_2}(\tau)$ with respect to the parameter τ.

$$D = \arg\max_{\tau} R_{s_1 s_2}(\tau) \tag{4}$$

By the Fourier transformation of $R_{s_1s_2}(\tau)$, the cross-spectral density (CSD) function $G_{s_1s_2}(\omega)$can be obtained. Namely, $R_{s_1s_2}(\tau)$and $G_{s_1s_2}(\omega)$ are the Fourier transform pair. The computation of the cross-correlation function is simpler in the frequency domain. Namely,

$$F\{R_{s_1s_2}(\tau)\} = G_{s_1s_2}(\omega) = aG_{ss}(\omega)e^{j\omega D} + G_{n_1n_2}(\omega) \tag{5}$$

where F is the Fourier transformation. If $n_1(t)$ and $n_2(t)$ are non-correlated, then $G_{n_1n_2}(\omega) = 0$. In this case, the cross-spectral density spectrum CSD, $G_{s_1s_2}(\omega)$, becomes the scaled version of $G_{ss}(\omega)$, multiplied by a complex exponential function. In practice, only the estimates $\hat{G}_{s_1s_2}(\omega)$ of $G_{s_1s_2}(\omega)$and $\hat{R}_{s_1s_2}(\tau)$ of $R_{s_1s_2}(\tau)$ can be obtained from the finite number of observations of signals $s_1(t)$ and $s_2(t)$. The Generalized Cross-Correlation function (GCC) is obtained by the inverse Fourier transformation of (5) as:

$$\hat{R}_{s_1s_2}(\tau) = \int_{-\infty}^{\infty} W(\omega)G_{s_1s_2}(\omega)e^{-j\omega\tau}d\omega \tag{6}$$

where $W(\omega)$ is a weight or window function. In order to smooth the estimated cross-correlation, various window functions can be used to make possible a more accurate estimation of time delay between signals. For smoothing, *ROTH, SCOT, PHAT, ECKART* [13] and other software packages can be used. The argument τ which maximizes the estimated $\hat{R}_{s_1s_2}(\tau)$ is ideally equal to the time delay D. Under ideal conditions, it is easy to exactly determine the location of the dominant peak (absolute maximum) of the cross-correlation function, i.e., to determine differential delay between the signals of the same source. The determination of the peak is impossible if the observation time for the cross-correlation function is unsatisfactory, especially in cases of small signal/noise ratios (SNR). When the cross-correlation function contains several multiple delays, the extraction of one peak becomes difficult. In practical applications, the signals have limited length and sources of noise are correlated, and in these cases, the cross-correlation function will not have a maximum at $\tau = D$.

The Coherence and Cramér-Rao lower bound

In general, the CSD function $G_{s_1s_2}(\omega)$, Eq. (5), has the form [19]:

$$G_{s_1s_2}(\omega) = \left|\gamma_{s_1s_2}(\omega)\right|[G_{s_1s_1}(\omega) \quad G_{s_2s_2}(\omega)]^{\frac{1}{2}} \tag{7}$$

It follows that:

$$\left|\gamma_{s_1s_2}(\omega)\right|^2 = C_{s_1s_2}(\omega) = \frac{\left|G_{s_1s_2}(\omega)\right|^2}{G_{s_1s_1}(\omega)G_{s_2s_2}(\omega)} \tag{8}$$

where $\gamma_{s_1s_2}(\omega)$ is the *spectral coherence function* for the signals $s_1(t)$ and $s_2(t)$, and $C_{s_1s_2}(\omega) = |\gamma_{s_1s_2}(\omega)|^2$ is the *magnitude square coherence function* – **MSC,** $G_{s_1s_2}(\omega)$and $G_{s_2s_2}(\omega)$are power spectral densities (PSD) of the signals $s_1(t)$ and $s_2(t)$, respectively. The spectral coherence function describes the degree of correlation between sensor signals on all the frequencies of interest. Seismic waves that are generated by the seismic source are propagated through a real world seismic medium to the sensors in the sensor array. If the sensor signals in the spatially distant geophones have a high level of spectral coherence in a rather wide spectral band, the peak in the cross-correlation peak will be significant and the differential time delay can be accurately determined [6]. The general Cramér-Rao lower bound (CRB) [13] for the variance of time delay estimation is:

$$CRB\left(\hat{D}\right) = \frac{2\pi}{T}\left(\int_{-\infty}^{\infty} \omega^2 SNR_{TD}(\omega)d\omega\right)^{-1} \tag{9}$$

where T is the observation period. Assuming that the coherence, signal and noise PSD are flat over a bandwidth $\Delta\omega$ centered at ω_0, and using the notation $G_{s_1s_1}(\omega) = G_{s_1s_1}$, $G_{s_2s_2}(\omega) = G_{s_2s_2}$, $G_{nn}(\omega) = G_{nn}$ and $\gamma_{s_1s_2}(\omega) = \gamma_{s_1s_2}$, from Eq. (9) the following equation is derived [6]:

$$CRB(D) = \left(2\omega_0\left(\frac{\Delta\omega\ \ T}{2\pi}\right)\left[1+\frac{1}{12}\left(\frac{\Delta\omega}{\omega_0}\right)^2\right]SNR_{TD}\left(\gamma_{s_1s_2}\right)\right)^{-1} \tag{10}$$

Threshold coherence

If the condition for the perfect coherence is not satisfied, i.e., if $|\gamma_{s_1s_2}(\omega)| \neq 1$, then the function $SNR_{TD}(\omega)$ characterizes the estimation performance. As shown in [24], the cross-correlation function of the narrow-band signal has a number of neighboring peaks (local maximums) with approximately the same magnitude (quasi-periodic function). In case of small SNR, the reliability of cross-correlation peak determination (corresponding to the true value of differential delay) decreases. The SNR value for coherent signals which delimits the regions of unreliable and reliable computation of differential delay (CR bound) is referred to as *SNR threshold* (SNR_{THRESH}). In other words, CRB is reachable if and only if $SNR_{TD}(\omega) \geq SNR_{THRESH}$. SNR_{THRESH} is defined by [20]:

$$SNR_{THRESH} = \frac{6}{\pi^2\left(\frac{\Delta\omega\ \ T}{2\pi}\right)}\left(\frac{\omega_0}{\Delta\omega}\right)^2\left[\phi^{-1}\left(\frac{1}{24}\left(\frac{\omega_0}{\Delta\omega}\right)^{-2}\right)\right]^2 \tag{11}$$

where:

$$\phi(y) = \frac{1}{2\pi}\int_y^{\infty} e^{-\frac{t^2}{2}}dt \tag{12}$$

ω_0 is the signal central frequency, $\Delta\omega$ is the signal bandwidth, T is the observation time, $(\Delta\omega T / 2\pi)$ is the time bandwidth product of the observations and $(\Delta\omega / \omega_0)$ is the fractional bandwidth (FB) of the signal. With partially coherent signals, instead of SNR_{THRESH}, THRESHOLD COHERENCE is defined [6]. If we define:

$$G_{s_1 s_1}(\omega) = G_{s_2 s_2}(\omega) = G_s \tag{13}$$

$$G_{n_1 n_1}(\omega_0) = G_{n_2 n_2}(\omega_0) = G_n \tag{14}$$

$$\gamma_{s_1 s_1}(\omega_0) = \gamma_s \tag{15}$$

The threshold coherence γ_s at the central frequency ω_0 can be represented as follows [6]:

$$\left|\gamma_s\right| = \left\{ \frac{\left[1 + \frac{G_n}{G_s}\right]^2}{1 + \frac{1}{SNR_{THRESH}}} \right\}^{\frac{1}{2}} \tag{16}$$

Kozick and Sandler [6] have shown that γ_s can be determined when SNR, the fractional bandwidth and the time-bandwidth product are specified, so that CRB bound of TDE is reached. Namely, the threshold coherence between non-coherent observed signals provides CRB at partially coherent signals. When the differential delay is computed for wideband signals, a certain degree of partial coherence can be tolerated while still providing CRB. Therefore, the partial coherence boundary which can still provide CRB is referred to as threshold coherence. From (16), one can conclude that the computation of threshold coherence makes sense only if $G_s / G_n = SNR_{THRESH}$. Thus, it is indirectly demonstrated that the threshold coherence depends on the same parameters as SNR_{THRESH}.

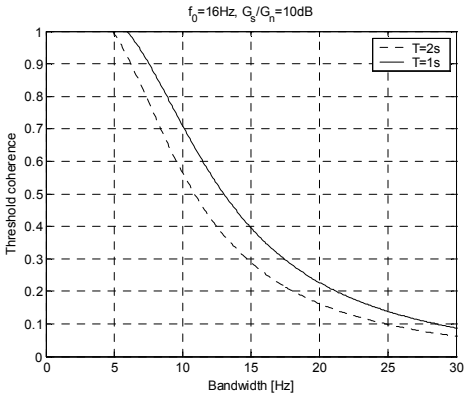

Fig. 1. The threshold coherence versus the signal bandwidth for $G_s / G_n = 10dB$, and $f_0 = 16Hz$.

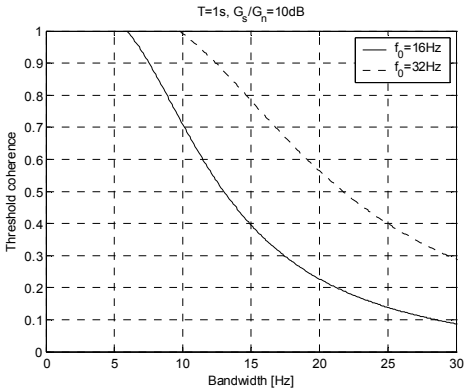

Fig. 2. The threshold coherence versus the signal bandwidth with G_s / G_n = 10*dB* and T=1*s*.

The parameters that have influence on the accuracy of the determination of the differential time delay of partially coherent signals are considered next. In the following figures, the functional dependence of the spectral coherence threshold (16) on a specific signal and observation parameters is shown. From Fig. 1, it can be observed that the threshold of coherence decreases with the increase of the observation time. For instance, for a characteristic seismic signal (obtained from geophone), having a central frequency $f_0 = 16Hz$, ($\omega_0 = 2\pi f_0$), $SNR=10dB$, $\Delta\omega = 2\pi 15 rad/sec$ and an observation time of T=1*s*, the threshold coherence is $\gamma_s \approx 0.4$. For the same signal parameters, when the observation time is increased to T=2*s*, the threshold coherence decreases to $\gamma_s \approx 0.3$ (Fig 1). Hence, one of the ways to decrease the threshold coherence is to increase the observation time of the signal, i.e., the length of the cross-correlation function (this way, quality criteria to reach CRB bound are relaxed). This way, the threshold coherence at stationary (non-moving) seismic sources can also be reduced. However, this approach is not suitable when seismic sources are moving, especially in geological media with small propagation velocities of seismic waves. For instance, the seismic surface R-wave propagation velocity varies from 100 *m/s* on the horizontal humus terrain to 6800 *m/s* in the marble [4].

The central frequency of the seismic signal also influences the coherence threshold of the observed signals (Fig. 2). Thus, the increase of the central frequency, when the bandwidth stays the same, leads to the increase of the coherence threshold. We've already observed that for a signal with the central frequency $f_0 = 16Hz$, $SNR = 10dB$, $\Delta\omega = 2\pi 15 rad/sec$, and observation time T=1*s*, the coherence threshold is $\gamma_s \approx 0.4$. If the central frequency increases to $f_0 = 32Hz$, the coherence threshold will be $\gamma_s \approx 0.8$ (Fig.2). These results can also be interpreted as follows: the coherence threshold decreases with increase of the bandwidth. Namely, for the aforementioned signals with the central frequency $f_o=32Hz$, the coherence threshold for the same bandwidth of $\Delta\omega = 2\pi 15 rad/sec$ is $\gamma_s \approx 0.78$. In contrast, for the signal with the same central frequency but $\Delta\omega = 2\pi 25 rad/sec$, the coherence threshold is $\gamma_s \approx 0.4$. The bandwidth/central frequency ratio $FB = \Delta\omega / \omega$ (a.k.a. fractional bandwidth - FB) has a significant influence on the coherence threshold (see Fig. 3). For instance, a signal with $FB = 0.5$, $SNR = 10dB$ and constant time-bandwidth product *Time x Bandwidth* = 100, has the coherence threshold $\gamma_s \approx 0.37$. From the same figure, one can conclude that the increase of *Time x Bandwidth*

product leads to a decrease of the coherence threshold. Naturally, this can be achieved either by an increase of the observation time or by an increase of the bandwidth. When the signal spectrum is wide enough, the decrease of coherence can be neglected when the differential delay is computed. In passive systems for localization, we may have an influence only on the observation time and not on the widening of the bandwidth. In contrast, in active localization systems we can vary both the central frequency and the bandwidth. Also, to neutralize the coherence loss, it is necessary to maintain a very large time-bandwidth product if the fractional bandwidth is small. Having in mind that the coherence threshold is computed based on SNR_{THRESH}-a, in Fig. 4 we demonstrate the SNR ratio threshold dependence on the bandwidth and the observation time. Thus, for the same bandwidth of $\Delta\omega = 2\pi 4 rad/s$, when the observation time is T=1s, the signal/noise ratio threshold is SNR_{THRESH} = 10dB, while for T=2s, SNR_{THRESH} = 20dB. This confirms the observation that the increase of the observation time decreases the threshold of SNR.

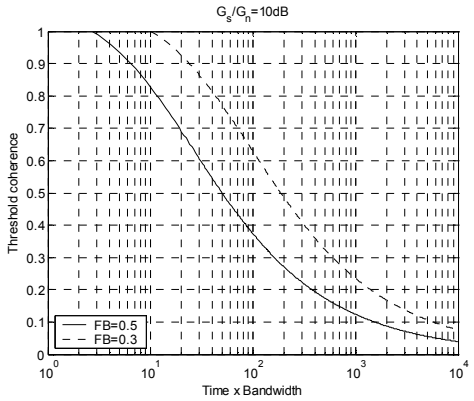

Fig. 3. The value of threshold coherence versus time-bandwidth product for $G_s / G_n = 10dB$

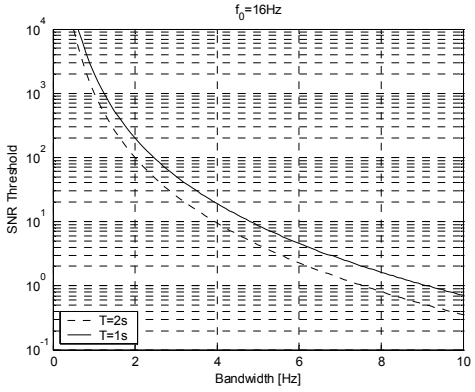

Fig. 4. The value of SNR threshold versus signal bandwidth with signal center frequency $f_0 = 16Hz$

S. Chow and P. M. Schultheiss [17, 18] have shown that the achievable mean-square error (MSE) in the ambiguity-dominated region is larger than CRB by factor $(\omega_0 / \Delta\omega)^2$. This result suggests the use of the signal envelope as the input to the cross-correlation. The signal envelopes do not have ambiguity problems associated with narrow-band signals. Hence, using them, we can expect to achieve MSE predicted by CRB with signal envelopes. To realize this idea, [18] proposes the combination of square-law envelope detectors and cross-correlators at the output of each sensor. In contrast, we propose to form an analytic signal prior to the computation of the cross-correlation function. This way, we prevent the ambiguity problem at the envelopes of correlated signals. In the rest of the paper, we will present the main characteristics of analytic signals and the methods of their generation. The advantages reached through the use of the signal envelope in numeric computation of differential delay are demonstrated on examples of deterministic and real acquired sensor signals.

3. SIGNAL (DATA) MODEL

Deterministic Analytic signal

To study in more detail the characteristics of the proposed estimator in the case of realistic and analytic signals, we modeled seismic signals. The seismic signal is modeled by deterministic complex exponential signals. The results of the simulated signals are confirmed on geophone signals from real-life acquisition. Golden [15] has studied the complex signals with the amplitude and phase functions varying in time. Such modeling has found applications in various fields including seismic signal processing. The visual representation of the waveforms of both simulated and real-life seismic signals in our system is given in Fig. 5 and Fig 6.

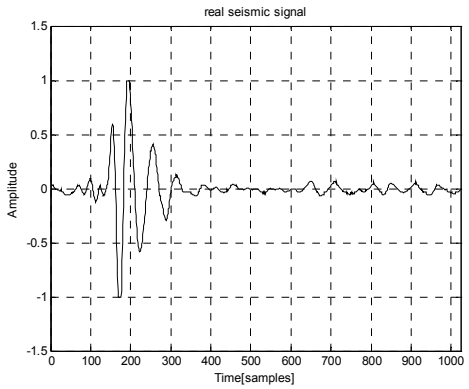

Fig. 5. The visual representation of the waveform of real-life seismic signal in our geophone sensor system.

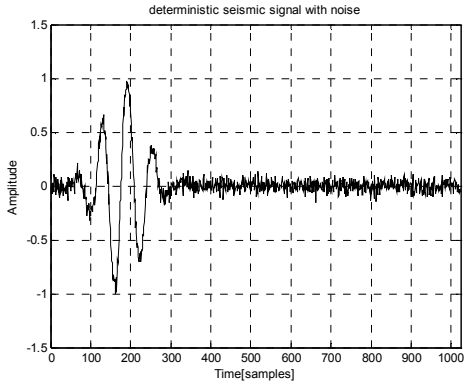

Fig. 6. The waveform of the real part deterministic signal obtained by (18), $a_0 = j\omega$, $a_1 = 0$, $a_2 = -2\alpha$, $\alpha = 200$ and $\omega = 2\pi 16 \text{rads}^{-1}$.

To verify the efficiency of the proposed algorithm on determination of differential delay, we simulated seismic signals using the analytic signal. The exponent of the waveform of the complex seismic signal can be approximately represented by a finite-degree polynomial [15]:

$$s(t) = \exp\left(a_0 + a_1 t + a_2 \frac{t^2}{2!} + \cdots\cdots + a_M \frac{t^M}{M!} \right) \quad , \quad a_i \in C, \quad i = 0,1,...,M \tag{17}$$

With seismic signals defined this way, the real and imaginary parts of analytic complex signals are related to. The real parts of coefficients of the polynomial (17) define the signal envelope, while the imaginary parts specify the signal phase. The main property of the analytic signal is that its Fourier transformation is zero for negative frequencies. Thus, the complex analytic signal has *one-side Fourier transform*, in other words, negative frequencies in the pharos representation of the spectrum are identical to zero.

The use of the analytic signal makes possible a simple computation of the current amplitude and phase values for each moment in time. If we assume that the real part of the complex analytic signal is in fact a real sequence identical to acquired real seismic signal, then the imaginary part of the complex analytic signal is the adjoin (corresponding) phase of the signal. The representation of the sensor signal by complex analytic sequence has important advantages in comparison to the presentation of the sensor signal by a real sequence, as is the case when "classic" GCC is computed. Namely, according to empirical evidence, the cross-correlation function of complex analytic signals is smooth and does not have the property of quasi-periodicity, unlike the cross-correlation function of signals represented by real sequences. In the presence of noise, the quasi-periodicity of the cross-correlation function can be a source of potential errors in computation of differential delay. To obtain an adequate simulate complex signal, the degree of the polynomial should be as large as possible. To simplify the analysis, here we assume the degree of 2. In our paper we apply the simplified analytic signal based on the second degree polynomial in the exponent, as follows:

$$s_n(t,\tau_n) = \exp(j\omega t - \alpha(t-\tau_n)^2) \tag{18}$$

where s_n *is the simulated analytic signal of n-th sensor*, $n = 1,2,3,...$ is the sensor identified, τ_n is absolute delay with respect to the origin in time ($t = 0$). By comparison of Eq. (17 and (18) the complex coefficients in (17) have the following values: $a_0 = 0 + j\omega$, $a_1 = 0$, $a_2 = -2\alpha + 0j$. During the simulation, the values of the parameters are $\alpha = 200$ and $\omega = 2\pi 16 \text{rads}^{-1}$ and the parameter τ_n is used to specify signal shifts with respect to the origin. By varying this parameter, it is possible to determine the differential delay between the simulated analytic signals. The pre-specified simulated differential delay $\Delta t_{n+1,n} = \tau_{n+1} - \tau_n$ is to be determined using the proposed technique based on the analytic signal. In this paper, the results are compared with the differential delay computed using the classic cross-correlation method based on *both* real and analytic signal. When comparing the Fourier coefficients for complex analytic and real seismic signals (consisting only of the real part of the complex analytic signal), the following can be observed:

- The real parts of the Fourier coefficients for positive frequencies of complex analytic signals are double the corresponding real parts of the Fourier coefficients signals which have only real components from complex analytic signals. This is the consequence of a real sequence representation as a sum of two conjugate complex phases and a complex sequence by only one pharos.
- The imaginary parts of the Fourier coefficients of a one-side complex analytic signal are equal to the corresponding imaginary parts of the Fourier coefficients of a signal that has only the real component of a complex analytic signal. Real and imaginary parts of a complex analytic signal are linked through the Hilbert transformation, so that the signal can be represented by only one pharos.

Analytic Signal from Real

The systems for seismic signal acquisition collect real seismic signals in the time domain. In [18], the computation of differential time delay using signal envelopes is suggested to prevent the ambiguity problem when the actual peak of the cross-correlation is computed. The property of analytic signals to have ideal complex envelopes is used in order to accomplish reliable computation of differential time delay. Thus, to apply the proposed GCC technique with analytic signals, it is necessary to transform real seismic signals into complex analytic signals. The resulting composite (transformed) complex analytic signal has a real part identical to the recorded real signal. In order to be analytic, the resulting complex signal must have its imaginary part related to its real part. Namely, the imaginary part of the analytic signals is the inverse Hilbert transformation of the real part of the analytic signal (or, equivalently, of the real part of the analytic signal). Thus, the imaginary part of the complex analytic sequence is a version of the original real sequence with a phase shift of $(\pi / 2)rad$.

$$s_{na}(t) = s_{nr}(t) + jH^{-1}[s_{nr}(t)] \tag{19}$$

where $s_{na}(t)$ is the analytic signal, $s_{nr}(t)$ is the real acquired signal and $H^{-1}(\bullet)$denotes the inverse Hilbert transform (in the time domain). This property of the Hilbert transformation is used to obtain an analytic signal based on the recorded real signal.

4. EXPERIMENTAL RESULTS

The estimation of differential delay between signals is performed using the GCC technique described in Section II. To simplify the computation, the window function from Eq. (6) is defined as: $W(\omega) = 1$. We begin our experimental evaluation on deterministic signals. First, we begin with complex analytic and then with real signals. Real signals correspond to signals from real-world systems for seismic source signal acquisition and localization. Finally, we will demonstrate results obtained on signals recorded in real settings. The waveform of the considered simulated complex analytic sensor signal is defined by Eq. (17) where the parameters have the following values: $a_0 = j2\pi 16$, $a_1 = 0$, $a_2 = -400$ and $a_3 = ... = a_M = 0$ (Fig. 6.). By specifying the signal shifts with respect to the start of the sequence using the parameter τ_n for n=1,2, we generate signals $s_1(t)$ and $s_2(t)$. The signals $s_1(t)$ and $s_2(t)$ have delays with respect to the origin of τ_1 and τ_2, respectively, hence the value of the simulated differential delay between $s_1(t)$ and $s_2(t)$ is $\Delta t_{2,1} = \tau_2 - \tau_1$. We assume $\tau_1 = 150$ *si* (sampling intervals), whereas τ_2 may take the values from a range that simulates the lag or lead of $s_2(t)$ with respect to $s_1(t)$. In a specific case, when $\tau_2 = \tau_1 = 150$ *si*, the signals are equal (if noise is not present) corresponding to the differential delay of $\Delta t_{2,1} = 0$. E.g., with $\tau_2 \langle \tau_1$, $s_2(t)$ leads with respect to $s_1(t)$, so that the differential delay is a negative value, $\Delta t_{2,1} \langle 0$. Moreover, with $\tau_2 \rangle \tau_1$, $s_2(t)$ is delayed with respect to $s_1(t)$, so that the differential delay is a positive value, $\Delta t_{2,1} \rangle 0$. By simultaneous sampling at sampling frequency of real and imaginary part of the analytic signal at *the* sampling frequency f_s=1*kHz*, we obtain a corresponding complex sequence $s_n(k)$, k=1,2,…N, which represents a sensor signal in the simulation. The parameter N, which actually corresponds to the length of the sequence vector, is in this case set to N=1024. When in simulation it is necessary to use only a real signal, we can take only the real part of the complex sequence. All the values of the parameters τ_1 and τ_2 are specified as integer multiples of the sampling interval (sampling period) si. Similarly, the computed values of the differential delay are specified as multiples of the sampling interval (period). In Fig. 7, we present the average absolute error of the computed differential delay $\Delta t_{2,1}$ between signals $s_1(t)$ and $s_2(t)$ for both real and complex signal representation. The absolute delay of signals $s_1(t)$ and $s_2(t)$ is determined by instant values of τ_1 and τ_2, respectively. The values of these parameters in Fig. 7, are $\tau_1 = const = 150si$ (sampling intervals), and $100si \leq \tau_2 \leq 300si$. Such choices of parameter values for τ_1 and τ_2 cover all characteristic relations between $s_1(t)$ and $s_2(t)$ in time domain (lags and leads). The experiment is performed such that the analytic signals $s_1(t)$ and $s_2(t)$ are generated for each pair of the parameters. The signals contain an additive Gaussian noise with zero mean such that SNR= 10dB. The experiments are repeated one hundred times and for each parameter pair $[\tau_1, \tau_2]$ the average absolute error of differential delay is computed.

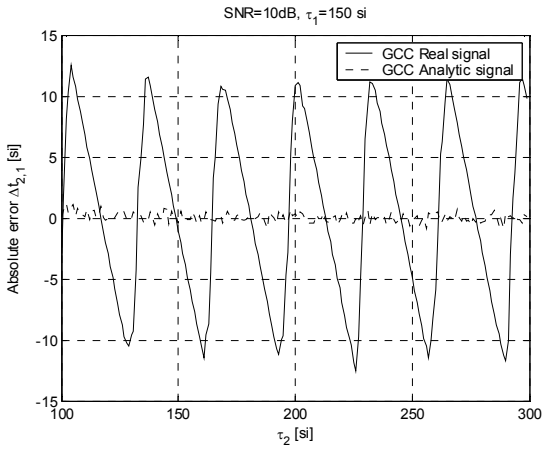

Fig. 7. The average absolute error of differential delay $\Delta t_{2,1}$ for analytic and real signals as function of parameter τ_2 (100 runs).

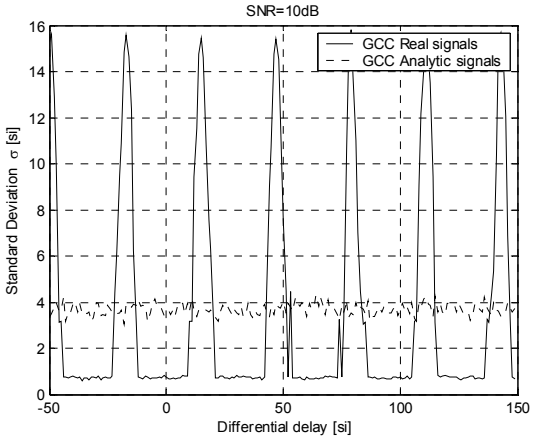

Fig. 8. The standard deviation of differential delay for analytic and real signals as function of differential delay (100 runs).

From Fig. 7, we can see that the numerical value of the estimation error $\Delta t_{2,1}$ for differential delay is very close to zero when $\tau_2 = 150si$. This is true both in cases of real and complex (analytic) representation of the signal. Further, it can be seen that the mean error, when the analytic signal representation is used, oscillates around zero and practically does not depend on the numerical value of τ_2. In contrast, when the real part of the signal is used, the error periodically changes the sign and has much larger amplitude. Hence, the

advantage of the proposed analytic representation in the differential delay estimation between two seismic signals is straightforward. When the actual signal is represented solely by the real portion of the analytic signal, from Fig. 7 it is evident that the absolute error of differential time delay estimation is much larger (up to 12 si). Such value of the absolute error is computed for the following parameter value $\tau_2 \approx 200$si. From Fig. 7, we can observe the periodicity of the absolute error, when the signal is represented only by its real part. This period of the absolute error is equal to the half of the simulated signal period, as it can be seen from Fig. 7. In Fig. 8, we show the standard deviation of the estimation error when differential delay is computed in experiments considered in Fig. 7. The figure illustrates the results for both real and complex analytic signals. Again, one can observe the periodicity of the standard deviation for real signals with respect to the true differential delay. This effect of periodicity cannot be observed for the standard deviation when the analytic signal is used.

In the rest of the paper, we analyze the results obtained when the proposed methods is applied on real-life signals. The real-life seismic signals are recorded from geophones situated in a real geological medium. The geophones are separated in space. The imaginary part of the signals is identically equal to zeros. Real seismic signals are acquired from two geophones that were laid on the surface at the same plane, and their distance was 20m. On the straight line defined by sensors, there was only one seismic source at the distance of 20m from the closer sensor. Signals from both sensors were collected with 1kHz sampling frequency, while the observation time was 1024 samples in order to apply the efficient FFT algorithm to compute the cross-correlation function. An anti-aliasing filter with the stopping frequency of 100Hz was at the entrance of the A/D converter.

In Fig. 9 we display cross-correlation functions of the real acquired signal of a geophone. The solid line is used to represent the cross-correlation as obtained by application of a classic GCC method with real signals, while the dashed line is used for the cross-correlation obtained when the GCC method is applied on complex analytic signals, as described in Section III. In these experiments, the differential time delay is determined by selection of the dominant peak in the corresponding cross-correlation function. Thus, the cross-correlation function which makes possible more reliable determination of the dominant peak also provides more confident numerical results of time delay estimation. GCC function (Fig. 9.) obtained from the analytic signal has a more clear peak and reduced ambiguity problem. The peak of the cross-correlation function is twice as large as the peak of the «classic» cross-correlation function, as obvious from Fig. 9. The numbers beside the peaks (abscises and ordinates) in Fig. 9, denote the numbers of samples where there is a maximal agreement between the observed signals and numerical values of peaks. Recall that based on the position of the peak, we can determine the differential delay between the signals $s_1(t)$ and $s_2(t)$. The coordinate of the peak of GCC function obtained with real signals is at sample 903, as well as the coordinate of the peak of the function computed using the analytic signals. Hence, in this particular case the two techniques have the same estimated values of time delays and the accuracy of the proposed method is preferable.

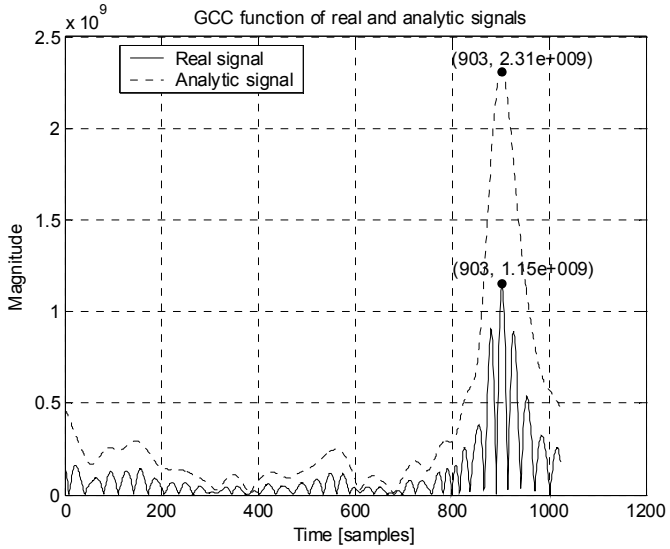

Fig. 9. The shape of the cross-correlation function obtained for experimental signals (the classic – solid and analytic-dash signal).

CONCLUSION

In this paper, we have described a powerful and efficient technique that applies complex polynomial analytic signals to determine the numerical value of differential delay of experimental seismic signals. The technique uses a novel smooth cross-correlation function that has a significant (dominant) peak and does not involve the use of classical prefilters [13]. We have presented a detailed analysis of classic real signals and the proposed analytic signals obtained through the Hilbert transformation in the frequency domain. We have considered and illustrated the errors when differential delay is computed and we have demonstrated the superiority of the proposed technique for the computation of the analytic signals cross-correlation. Open research problems are related to the quality of the experimental signals at the input, design of a new generation of sensors and simultaneous acquisition of all the signals from an active sensor cell with a higher resolution and sampling frequency. In addition, the research of efficient algorithms for source localization can significantly improve the applications in systems for real-time passive source localization. Our work in progress with the proposed estimator for the cross-correlation function of analytical signals is focused on:

- reduction of the influence of a non-homogeneous geological medium and multipath effects on differential delay computation,
- determination of seismic, sonar and acoustic source trajectories,
- detection of the number of active sources in the domain of the sensor cell and their tracking in real time,

- identification and classification of seismic, sonar and acoustic sources,
- determination of the optimal geometry of the sensor cell network of spatially separated geophones and
- optimization of inter-sensor and inter-network communication needs for source localization by the collaborative sensor arrays.

REFERENCES

1. E. R. Seriff, P. L. Geldfart, "Exploration Seismology", Vol. History, theory & data acquisition, *Cambridge University Press*, 1986.
2. J. Chen, J. Benesty, Y. Huang, "Time delay estimation in room acoustic environments: an overview", *EURASIP Journal on Applied Signal Processing,* pp. 1-19, 2006.
3. V. D. Pavlović, Z. S. Veličković, "Measurement of Seismic Waves Propagation Velocity in the Real Medium", *The scientific journal "FACTA UNIVERSITATIS" Series: Physics, Chemistry and Technology.* Vol. 1, N° 5, 1998 pp. 63-73, NIŠ 1998, *http://www.facta.junis.ni.ac.yu.*
4. S. Golden, B. Friedlander, „Maximum Likelihood Estimation, Analysis, and Applications of Exponential Polynomial Signals", *IEEE Trans. Signal Processing*, vol. 47, pp.1493-11501, June 1999.
5. V. D. Pavlović, Z. S. Veličković, "Explicit Form Localizing of Unknown Source of Seismic Vibrations", *The International Conference on Signal Processing Applications and Technology – ICSPAT,* pp. 1097-1104, San Diego, CA, 1997.
6. R. J. Kozick, B. M. Sadler, „Source Localization With Distributed Sensor Arrays and Partial Spatial Coherence", *IEEE Trans. Signal Processing*, vol. 52, pp.601-616, March 2004.
7. X. Sheng Y. Hu, „Maximum Likelihood Multiple-Source Localization Using Acoustic Energy Measurements with Wireless Sensor Networks", *IEEE Trans. Signal Processing*, vol. 53, pp.44-53, January 2005.
8. G. Papadopoulos, K. Efstathiou, Yigi Li, „Implementation of Intelligent Instrument for Passive Recognition and Two-Dimensional Location Estimation of Acustic Targets", *IEEE Trans. On Instrumentation and Measurement*, vol. 41, pp.885-890, December 1992.
9. H. Jeong, Y. Jang, „Fracture Source Location in Thin Plates Using the Wavelet Transform of Dispersive Waves", *IEEE Trans. Ultrasonic, Ferroelectrics and Frequency Control*, vol. 47, pp.612-619, May 2000.
10. A. B. Gershman V. I. Turchin, V.A. Zverev, „Experimental Results of Localization of Moving Underwater Signal by Adaptive Beamforming", *IEEE Trans. Signal Processing*, vol. 43, pp.2249-2257, October 1995.
11. A. B. Gershman, C. F. Mecklenbrauker, F. Bohme, „Matrix Fitting Approach to Direction of Arrival Estimation with Imperfect Spatial Coherence of Wavefronts", *IEEE Trans. Signal Processing*, vol. 45, pp.1894-1899, July 1997.
12. S. A. Vorobyov, A. B. Gershman, K. M. Wong, „Maximum Likelihood Direction-of-Arrival Estimation in Unknown Noise Fields Using Sparse Sensor Arrays", *IEEE Trans. Signal Processing*, vol. 53, pp.34-42, January 2005.
13. C. H. Knap G. C. Carter, „The generalized Correlation Method for Estimation of Time Delay", *IEEE Trans. Acoust., Speech, Signal Processing*, vol. ASSP-24, pp.320-327, August 1976.
14. J. C. Hassab, R.E. Boucher, „Optimum estimation of Time Delay by a Generalized Correlator", *IEEE Trans. Acoust., Speech, Signal Processing*, vol. ASSP-27, pp.979-380, August 1979.
15. U. Spagnolini, „Nonparametric Narrowband Wavefront Estimation from Wavefront Gradients", *IEEE Trans. Signal Processing*, vol. 47, pp.3116-3121, January 2005.
16. A. G. Piersol, „Time delay Estimation using Phase Data", *IEEE Trans. Acoust., Speech, Signal Processing*, vol. ASSP-29, pp.471-477, June 1981.
17. P. M Schultheiss, E. Weinstein, „Lower Bounds on the Localization Errors of a Moving Source Observed by a Passive array", *IEEE Trans. Acoust., Speech, Signal Processing*, vol. ASSP-29, pp.600-607, June 1981.
18. S. Chow, P. M Schultheiss, "Delay Estimation Using Narrow-Band Processes", *IEEE Trans. Acoust., Speech, Signal Processing*, vol. ASSP-29, pp.478-484, June 1981.
19. K. Scarbrough, N. Ahmed, G.C.Carter., "On the simulation of a class of Time Delay Estimation Algorithms", *IEEE Trans. Acoust., Speech, Signal Processing*, vol. ASSP-29, pp.534-539, June 1981.
20. A. J. Weis, E. Weinstein, "Fundamental Limitations in Passive Time Delay Estimation-Part I: Narrow-Band Systems", *IEEE Trans. Acoust., Speech, Signal Processing*, vol. ASSP-29, pp.472-486, April 1983.
21. P. Costa, J. Gouffaud, P. Larzabal, „Estimation of the Number of Signals from Features of Covariance Matrix: A Supervised Approach", *IEEE Trans. Signal Processing*, vol. 47, pp.3108-3115, November 1999.

22. B. Emile, P. Comon, J. L. Roux, „Estimation of Time Delays with Fewer Sensors than Sources“, *IEEE Trans. Signal Processing*, vol. 46, pp.2012-2015, July 1998.
23. L. N. Chrysostomas., P. P. Atina, “Higher-order spectra analysis", PTR Prentice-Hall, inc., 1993.
24. J. Wen, P. Li, “A new method for unbiased time-delay estimation in noisy environments", *Int. J. Adapt. Control Signal Process*, DOI: 10.1002/acs.951, 2007.

PRIMENA KOMPLEKSNIH ANALITIČKIH SIGNALA U IZRAČUNAVANJU VREMENSKOG KAŠNJENJA

Zoran S. Veličković, Vlastimir D. Pavlović

U ovom radu je prezentovan koncept izračunavanja diferencijalnog kašnjenja koji je zasnovan na transformaciji realnog senzorskog signala u analitički. Analizirane su vrednosti dobijenih diferencijalnih kašnjenja za realni seizmički signal, simulirani kompleksni analitički signal i simulirani kompleksni analitički signal čiji realni deo odgovara akviziranom realnom signalu. Simulacioni rezultati pokazuju da se primenom kompleksnog analitičkog signala dobijaju pouzdanije vrednosti diferencijalnog kašnjenja. Analiziran je uticaj specifičnih parametara signala na prag koherence u sistemima za pasivnu lokalizaciju i preporučeni su metodi za njeno snižavanje. Diferencijalno vreme kašnjenja je određeno u odnosu na referentni senzor (geofon) primenom GCC metoda nad analitičkim signalima. Poteškoće oko određivanja pika kros-korelacione funkcije kod realnih signala, koji odgovara tačnom diferencijalnom kašnjenju, su znatno redukovane primenom GCC metoda nad analitičkim signalima. Efikasnost predložene tehnike je ispitana na determinističkim i realnim signalima.